

Single-Molecule Graphene Junction Aflatoxin Sensors: Chemo-Physical Insights from Ab Initio Simulations

Original

Single-Molecule Graphene Junction Aflatoxin Sensors: Chemo-Physical Insights from Ab Initio Simulations / Mo, Fabrizio; Ala, Walter; Spano, Chiara Elfi; Piccinini, Gianluca; Graziano, Mariagrazia; Ardesi, Yuri. - ELETTRONICO. - (2024), pp. 420-423. (2024 IEEE 24th International Conference on Nanotechnology (NANO) Gijon (Spain) 08-11 July 2024) [10.1109/nano61778.2024.10628920].

Availability:

This version is available at: 11583/2991938 since: 2024-09-11T13:49:22Z

Publisher:

IEEE

Published

DOI:10.1109/nano61778.2024.10628920

Terms of use:

This article is made available under terms and conditions as specified in the corresponding bibliographic description in the repository

Publisher copyright

IEEE postprint/Author's Accepted Manuscript

©2024 IEEE. Personal use of this material is permitted. Permission from IEEE must be obtained for all other uses, in any current or future media, including reprinting/republishing this material for advertising or promotional purposes, creating new collecting works, for resale or lists, or reuse of any copyrighted component of this work in other works.

(Article begins on next page)

Single-Molecule Graphene Junction Aflatoxin Sensors: Chemo-Physical Insights from Ab Initio Simulations

Fabrizio Mo*, Walter Ala*, Chiara Elfi Spano*, Gianluca Piccinini*, Mariagrazia Graziano[†], Yuri Ardesi*[‡]
*Department of Electronics and Telecommunications, Politecnico di Torino, Torino, Italy
[†]Department of Applied Science and Technology, Politecnico di Torino, Torino, Italy
[‡]corresponding author e-mail: yuri.ardesi@polito.it

Abstract—The aflatoxin B1 (AFB1) is a cancerogenic compound affecting the agri-food chain, endangering food safety and public health. Worldwide regulatory agencies establish strict limitations for the presence of AFB1 in crops. Current detection methods require bulky equipment, long measurement time, and skilled laboratory researchers, which make it challenging to measure the AFB1 in the whole food chain pervasively. In this field, molecular junctions represent an exciting alternative in the sensing application, providing a highly integrable device for the fast measurement of chemical compounds. Through *ab initio* simulation, this work investigates graphene junctions for detecting AFB1. The results show that applying a bias voltage of 1.2 V to a graphene layer permits varying the electrical current of the junction by more than 3 μ A when the AFB1 is present. The obtained results motivate research on the integrability of the device in more complex sensing systems such as intelligent sensors and electronic noses.

I. INTRODUCTION

The aflatoxins are a group of oncogenic mycotoxins primarily produced by the *Aspergillus Flavus* and the *Aspergillus Parasiticus*, which contaminate crops, such as peanuts, corn, and nuts, producing serious effects on human and animal health [1]. The aflatoxin B1 (AFB1) has been inserted in *Group 1* of cancerogenic compounds [2]. Regulatory agencies worldwide established strict limitations for the presence of AFB1 in crops to guarantee food safety and mitigate adverse effects on public health.

In this context, the measurement of AFB1 is crucial. Measurement laboratories typically exploit techniques such as High-Performance Liquid Chromatography (HPLC), providing precise quantification, and Enzyme-Linked Immunosorbent Assay (ELISA) for fast measurement. However, the mentioned methods require bulky equipment, long measurement time, and skilled laboratory researchers, which make it challenging to apply these methods in the whole food chain pervasively. Recently, researchers proposed using molecular junctions to fabricate single-molecule sensors, providing a highly integrable device for the fast measurement of chemical compounds [3]–[5]. Fig. 1(a) shows the general structure of a single-molecule sensor. A molecule is sandwiched between two electrodes, named source (S) and drain (D), creating a molecular channel whose conductive properties are sensible to the presence of other molecules. The sensor sensitivity can

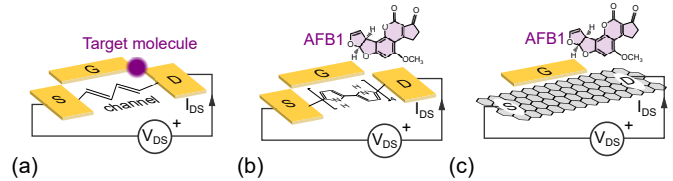


Fig. 1. Single-molecule sensors: (a) basic schematic of single-molecule sensors composed of a molecular channel and two electrodes, S and D, used for detecting the target molecule through amperometric measurement. A possible gate electrode G permits sensitivity improvement, (b) basic schematic of the AFB1 single-molecule sensor proposed in [7] made up with a gold-8-Pyrrole-DiThiol-gold junction with a gate structure, (c) proposed graphene sensor.

eventually be engineered by acting on a third electrode, gate (G), which permits sensitivity modulation [6].

Fig. 1(b) shows the single-molecule sensor proposed in [7] for the measurement of AFB1. A gate electrode is added to engineer the molecular sensor and improve the sensitivity [6]. In particular, we demonstrate in [7], [8] that a well-engineered gold-8-Pyrrole-DiThiol-gold junction permits the detection of AFB1 molecule. Indeed, the electrical current results decreased by 80% when the target molecule reached the polymeric channel. In this work, we investigate through *ab initio* simulation the use of graphene junctions for AFB1 detection. Graphene, indeed, has already shown promising results in the field of sensing small quantities in its functionalized form [9], and carbon allotropes have been used in [10] as functionalization elements for portable aflatoxin M1 biosensors. Fig. 1(c) shows the proposed device with the AFB1 target molecule. In particular, this work focuses on exploiting graphene channels to realize single-molecule junctions based on carbon allotropes. Graphene contains only carbon atoms, which present valence electrons free to interact with target molecules. In addition, the 2D nature of the graphene makes it promising for the realization of organic electronic noses [11].

Graphene promises high sensitivity of the final sensor since variations of the surface conductive properties are directly reflected in the sensor conduction. Surface properties, responsible for the sensing mechanism, are maximized compared to the overall volume of graphene. This work shows preliminary

results that demonstrate the capability of graphene junctions to modulate their conduction when exposed to AFB1. Our outcomes motivate further research in developing graphene and single-molecule sensors for sensing small molecules and realizing future smart sensors and electronic noses.

II. METHODOLOGY

This study investigates the use of graphene junctions for detecting AFB1 molecules. We use Synopsis QuantumATK [12] to assess the adsorption energy of AFB1-graphene configurations. The *ab initio* calculation is performed in the framework of the Density Functional Theory (DFT) by employing the GGA/PBE computational method with Grimme DFT-D3 correction, PseudoDojo medium pseudopotential and basis set, along with counterpoise correction. Periodic boundary conditions are employed for the transport-transverse direction to simulate the graphene layer, while Dirichlet boundary conditions are applied elsewhere.

Ab initio calculation examines the adsorption of AFB1 on the *ab initio*-relaxed graphene layer, permitting determining the most probable configuration of the AFB1 molecule on the graphene surface. The AFB1 molecule is positioned at multiple points and with several orientations on the graphene layer, and the energy of the graphene+AFB1 system (E_{TOT}) is computed with QuantumATK by relaxing the entire system geometry through the LBFGS algorithm with a force tolerance of 0.05 eV/Å. The adsorption energy (E_{ADS}) for all configurations is calculated as:

$$E_{ADS} = E_{TOT} - (E_G + E_{AF}) \quad (1)$$

where E_G and E_{AF} represent the energy of graphene and AFB1, respectively. The configuration with the lowest energy is considered the most probable, as it minimizes E_{TOT} .

To assess the transport properties of the junction, QuantumATK is again used to evaluate the junction current. In nanoscale devices, the current can be described by the Landauer formula [13]:

$$I_{DS} = \frac{2q}{h} \int_{-\infty}^{+\infty} T(E, V_{DS}) [f_S(E) - f_D(E)] \quad (2)$$

where q is the electron charge, h is the Planck constant, f_S and f_D are the Fermi-Dirac distributions, and T is the transmission spectrum, which depends on the electron energy (E), and the bias voltage (V_{DS}). T is calculated with the quantum mechanical Non-Equilibrium Green's Function (NEGF) theory, as detailed in [12], [13].

III. RESULTS AND DISCUSSION

This section examines the graphene junction aflatoxin sensor using *ab initio* calculation. Firstly, it investigates the geometries of the molecular species involved in the study, namely graphene and AFB1, to analyze AFB1 adsorption on graphene and determine the most probable configurations. Secondly, it explores the transport properties of the most

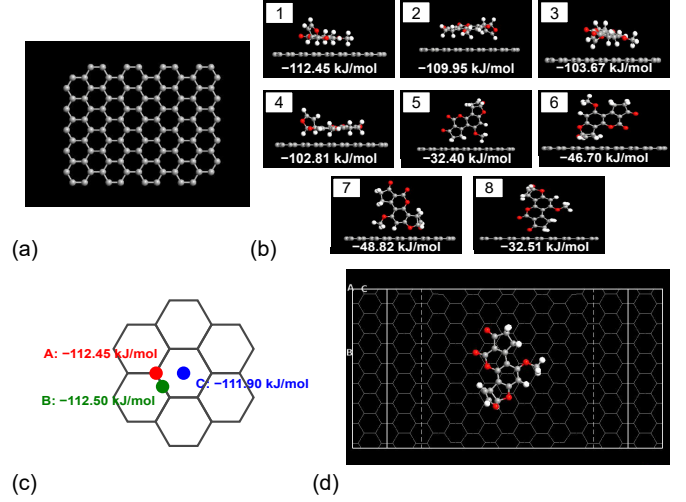


Fig. 2. Graphene junction aflatoxin sensor: (a) graphene layer obtained from the *ab initio* geometry optimization, (b) studied adsorption configurations of the AFB1 on graphene with adsorption energies, (c) different adsorption sites used for the aflatoxin in *Configuration 1* to study adsorption site dependence, (d) device configuration used for the transport *ab initio* study.

stable configuration, namely *Configuration 1*, to gain precise insights into the sensor behavior and understand the physics of AFB1-graphene interaction. Finally, the section investigates the transport properties of the second most stable configuration, namely *Configuration 2*, to evaluate the robustness of the presented methodology and to assess the potential measurement variations expected in field use.

A. Study of the adsorption configuration

This section studies the *ab initio* geometry relaxation of the involved species, i.e., the graphene and the AFB1 molecule. The relaxation is fundamental for accurately studying the adsorption of AFB1 onto the graphene layer and consequently evaluating the transport properties and the sensing mechanism.

Fig. 2(a) shows the graphene layer obtained through *ab initio* geometry relaxation, essential for correct study of AFB1 adsorption and energy evaluation. The size of the graphene layer, consisting of 40 hexagons, is chosen to prevent AFB1 from exceeding the graphene edges during adsorption. After geometry relaxation, the aflatoxin molecule is positioned 0.2 nm far from the graphene layer in 8 possible configurations, i.e., with different rotations. This configuration is also relaxed to find the minimum energy configuration. Fig. 2(b) depicts the analyzed configurations and their corresponding adsorption energies (E_{ADS}). *Configuration 1* demonstrates the lowest adsorption energy ($E_{ADS} = -112.4508$ kJ/mol), indicating strong physisorption of AFB1 onto the graphene layer. The study is also repeated by slightly changing the molecule position, depicted in Fig. 2(c), by positioning AFB1 above a carbon atom (A), in the center of a bond (B) or in the center of a hexagon (C). The energy variation is minimal, denoting a feeble dependence of the adsorption energy on the site.

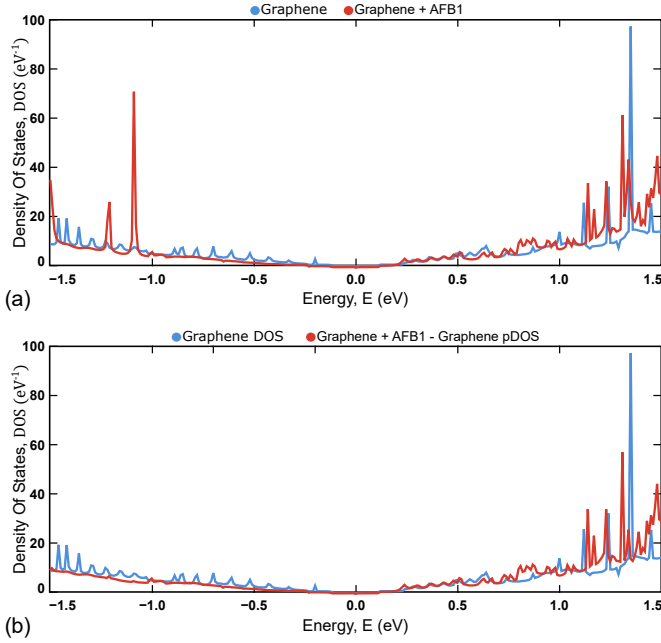


Fig. 3. Density of states (DOS) of the graphene junction aflatoxin sensor: (a) DOS of the device with and without the aflatoxin molecule, (b) Comparison between the DOS of the graphene junction device, without the aflatoxin, and of the DOS of the graphene junction device, with aflatoxin, projected on the graphene layer, i.e. the projected DOS.

B. Transport properties of the most stable configuration

Configuration 1, the lowest energy configuration, is used to construct the device. An *ab initio* calculation analyzes the device electrical transport with and without AFB1.

Fig. 2(d) shows the device configuration created in QuantumATK to study the electrical properties. The graphene layer for the transport analysis is enlarged to 91 hexagons to reduce the interaction between AFB1 and electrodes in the transport direction, and the complete geometry is again relaxed with the *ab initio* geometry optimization tool.

Fig. 3(a) shows the device density of states (DOS) of graphene with and without the AFB1 molecule, here referred to as naked and exposed DOS, respectively. The presence of AFB1 introduces two peaks with negative energies around -1.1 eV and -1.2 eV in the exposed DOS, indicating potential variations in sensor transmittivity due to AFB1. Additionally, Fig. 3(b) depicts the projected DOS (pDOS) of the graphene junction in the presence of AFB1, compared to the graphene DOS, which highlights the influence of AFB1 on the graphene junction, thus affecting the junction conductive properties. Specifically, the pDOS is lower than the naked DOS, suggesting a reduction in junction conduction states when exposed to AFB1. Notably, in a molecular junction, the current generally depends on the broadening of states rather than their presence. The broadening arises from the molecular bonding to the contact. The DOS consists of delta Dirac distributions that change into Lorentzian distributions when the single molecule is connected to electrodes. The broadening reflects the delocalization of electrons on the graphene channel. A high broadening leads to increased

device transmittance and final junction current.

To better investigate the conduction properties, it is worth study the transmission spectrum of the graphene junction with and without the AFB1. Fig. 4(a) shows the transmission spectrum (T) evaluated at the equilibrium ($V_{DS} = 0$ V). The variation in the transmittivity, when AFB1 is present, permits the modulation of the conductivity and, thus, the sensing mechanism. Generally, AFB1 presence leads to a slight increase of T for positive energies and a decrease for negative ones. Attenuated T peaks are also present for deeply positive energies. Fig. 4(b) shows the I/V characteristics evaluated by applying a voltage (V_{DS}) to the junction. For small bias (close to 0 V), the current modulation in the presence of AFB1 is minimal. There is agreement with the previous result: T variations are compensated for energies around 0 eV in the Landauer's integral (equation 2), and negligible current variation appears. Instead, the AFB1 significantly reduces the current by $3.167 \mu\text{A}$ when applying a bias voltage of $V_{DS} = 1.2$ V. Since the considered V_{DS} is significantly different from 0 V (equilibrium) and since $T(E, V_{DS})$ is a function of both E and V_{DS} , to explain the reasons of such current reduction, we must consider $T(E, V_{DS} = 1.2$ V). Fig. 4(c) shows the transmission spectrum evaluated at $V_{DS} = 1.2$ V, which highlights the lowering of transmittivity in the bias window, i.e., in the $[-0.6, 0.6]$ eV range, associated to the applied voltage $V_{DS} = 1.2$ V. From a physical perspective, we relate the current decrease to the perturbation of the electron transmission in the graphene layer caused by the AFB1 presence. Fig. 5 shows the junction transmission eigenstates in the presence of AFB1. The transmission eigenstates are a real-space projection of the solutions for the transmission operator eigenproblem. Their bright areas in Fig. 5 highlight the transmission perturbation on the graphene layer due to the AFB1, in contrast with the homogeneous transmission present far away from the AFB1, thus demonstrating AFB1-induced scattering.

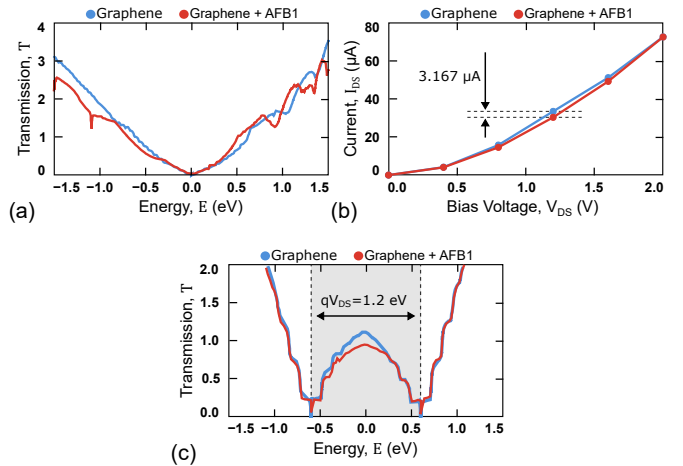


Fig. 4. Transport study on *Configuration 1*: (a) transmission spectrum, (b) I/V characteristics of the graphene sensor, (c) transmission spectrum evaluated at $V_{DS} = 1.2$ V.

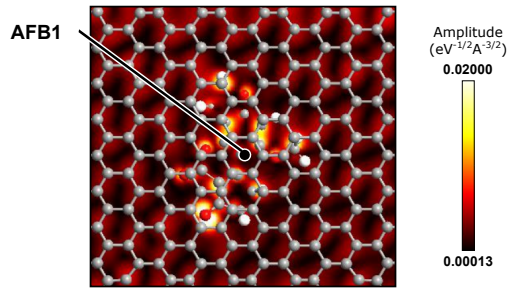


Fig. 5. Eigenstates of the graphene junction aflatoxin sensor with the AFB1 molecule.

C. Transport properties of the second most stable configuration

The previous section studies the most stable configuration of the proposed device, as it is the one demonstrating the lowest energy and, thus, the most probable at the thermal equilibrium. As the final study of this work, following the same procedure used for *Configuration 1*, this section investigates transport properties of *Configuration 2* to evaluate the robustness of the proposed methodology and the expected variations in the sensor current when the device is used in a real scenario. Indeed, it is possible supposing that the AFB1 molecule will move its position in space due to thermal noise.

Configuration 2, previously shown in Fig. 2(b), involves a 90-degree rotation of the molecule on the graphene layer. The adsorption energy, $E_{ADS} = -109.95$ kJ/mol, remains comparable to the one of *Configuration 1*, with a small increase of 2.5 kJ/mol. Fig. 6 shows the current evaluated with *Configuration 2* and compare it with the isolated graphene and *Configuration 1*. Notably, the current trend resembles the one observed in *Configuration 1*. For the bias voltage $V_{DS} = 1.2$ V, the current is slightly increased by $0.650 \mu\text{A}$, which is still limited concerning the current in the naked sensor. The margin is reduced to $2.511 \mu\text{A}$.

The voltage bias point $V_{DS} = 1.2$ V is confirmed as the optimal sensitivity point for the detection of the AFB1 molecule, despite the assumed configuration, giving a first proof regarding the possibility of exploiting single-molecule graphene junctions for the detection of the AFB1.

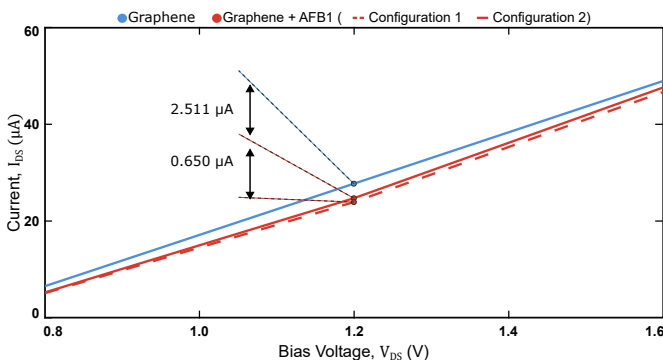


Fig. 6. Current evaluated for the graphene junction aflatoxin sensor in *Configuration 2*.

IV. CONCLUSION

This work demonstrates the applicability of graphene junctions for realizing Aflatoxin B1 (AFB1) single-molecule sensors. The results show that AFB1 adsorbs on graphene in stable configurations and that AFB1 produces scattering in the graphene layer, thus affecting transmission properties and reducing the junction electrical current. In particular, applying a bias voltage of 1.2 V to a graphene layer permits varying the electrical current of the junction by $3.167 \mu\text{A}$ when the AFB1 is present. The obtained value is measurable with electronic equipment, enabling the future realization of an integrated electronic system to detect aflatoxin in the agri-food chain pervasively. Further works will investigate the sensor selectivity concerning other molecules present in practical cases, the realization of the single-molecule sensors based on different carbon allotropes, and the experimental validation of the obtained results. Finally, the results motivate further work to address the device integrability in more complex sensing systems such as electronic noses.

REFERENCES

- [1] M. Edite Bezerra da Rocha, F. da Chagas Oliveira Freire, F. Erlan Feitosa Maia, M. Izabel Florindo Guedes, and D. Rondina, "Mycotoxins and their effects on human and animal health," *Food Control*, vol. 36, no. 1, pp. 159–165, 2014.
- [2] IARC Working Group on the Evaluation of Carcinogenic Risks to Humans, "Some traditional herbal medicines, some mycotoxins, naphthalene and styrene," *IARC Monogr Eval Carcinog Risks Hum*, vol. 82, pp. 1–556, 2002.
- [3] Y. Li, C. Yang, and X. Guo, "Single-molecule electrical detection: A promising route toward the fundamental limits of chemistry and life science," *Accounts of Chemical Research*, vol. 53, no. 1, pp. 159–169, 2020. PMID: 31545589.
- [4] J. J. Gooding and K. Gaus, "Single-molecule sensors: Challenges and opportunities for quantitative analysis," *Angewandte Chemie International Edition*, vol. 55, no. 38, pp. 11354–11366, 2016.
- [5] F. Mo, Y. Ardesi, M. R. Roch, M. Graziano, and G. Piccinini, "Investigation of amperometric sensing mechanism in gold-c60-gold molecular dot," *IEEE Sensors Journal*, vol. 22, no. 20, pp. 19152–19161, 2022.
- [6] F. Mo, C. E. Spano, Y. Ardesi, M. Ruo Roch, G. Piccinini, and M. Graziano, "Design of pyrrole-based gate-controlled molecular junctions optimized for single-molecule aflatoxin b1 detection," *Sensors*, vol. 23, no. 3, 2023.
- [7] F. Mo, C. E. Spano, Y. Ardesi, M. R. Roch, G. Piccinini, and M. Graziano, "Single-molecule aflatoxin b1 sensing via pyrrole-based molecular quantum dot," in *2022 IEEE 22nd International Conference on Nanotechnology (NANO)*, pp. 153–156, 2022.
- [8] F. Mo, Y. Ardesi, C. E. Spano, M. R. Roch, G. Piccinini, and M. Graziano, "Effect of adsorption mechanism on conduction in single-molecule pyrrole-based sensor for afb1," *IEEE Transactions on Nanotechnology*, vol. 22, pp. 811–816, 2023.
- [9] R. Campos, J. Borne, J. R. Guerreiro, G. Machado, Jr, M. F. Cerqueira, D. Y. Petrovykh, and P. Alpuim, "Attomolar label-free detection of DNA hybridization with electrolyte-gated graphene field-effect transistors," *ACS Sens.*, vol. 4, pp. 286–293, Feb. 2019.
- [10] B. D. Abera, A. Falco, P. Ibba, G. Cantarella, L. Petti, and P. Lugli, "Development of flexible dispense-printed electrochemical immunosensor for aflatoxin M1 detection in milk," *Sensors (Basel)*, vol. 19, p. 3912, Sept. 2019.
- [11] A. Parichenko, S. Huang, J. Pang, B. Ibarlucea, and G. Cuniberti, "Recent advances in technologies toward the development of 2D materials-based electronic noses," *Trends Analyt. Chem.*, vol. 166, p. 117185, Sept. 2023.
- [12] S. Smidstrup *et al.*, "QuantumATK: an integrated platform of electronic and atomic-scale modelling tools," *Journal of Physics: Condensed Matter*, vol. 32, p. 015901, oct 2019.
- [13] S. Datta, *Quantum Transport: Atom to Transistor*. Cambridge University Press, 2005. doi: 10.1017/CBO9781139164313.